*Polymer* Vol. 37 No. 11, pp. 2243–2250, 1996
Copyright © 1996 Elsevier Science Ltd
Printed in Great Britain. All rights reserved
0032-3861/96/$15.00+0.00

# Permeability of co-extruded linear low-density polyethylene films to oxygen and carbon dioxide as determined by electrochemical techniques

**Vicente Compañ**
*Departmento de Física, Universidad Jaume I, 12080 Castellón, Spain*

**and Amparo Ribes and Ricardo Díaz-Calleja**
*Departamento de Termodinámica Aplicada, UPV, 46020 Valencia, Spain*

**and Evaristo Riande***
*Instituto de Ciencia y Technologíca de Polímeros (CSIC), 28006 Madrid, Spain*
*(Received 26 October 1994; revised 22 February 1995)*

The mechanical relaxation spectra of co-extruded linear low-density polyethylene (LLDPE) films, prepared from copolymers of ethylene and 1-octene, were measured in parallel and transverse directions to the processing orientation. Both the $\gamma$- and $\beta$-relaxations do not show a noticeable dependence on the direction in which the measurements were performed. However, whereas the $\alpha$-relaxation in the measurements performed in the parallel direction appears as two peaks, in order of increasing temperature, which were denoted as $\alpha'$ and $\alpha''$, the measurements carried out in the transverse direction only exhibit the $\alpha'$-peak. The influence of tensile drawing on the permeability of co-extruded LLDPE films to oxygen and carbon dioxide was investigated by electrochemical techniques over the range of temperatures where the $\alpha'$-relaxation process is located. In general, the permeability coefficients do not show a significant dependence on the drawing direction in the temperature interval corresponding to the low-temperature region of the $\alpha'$-peak. In this high-temperature zone, the values of the permeability coefficient for $O_2$ and $CO_2$ through the oriented films after tensile drawing are significantly lower than those obtained for these gases through undrawn co-extruded LLDPE films. The diffusion coefficients do not show a definite dependence on tensile drawing.
Copyright © 1996 Elsevier Science Ltd.

**(Keywords: linear LDPE; permeability; dynamic mechanical relaxation)**

## INTRODUCTION

Permeation of gases through polymer films involves dissolution of the gas at the high-pressure interface, molecular diffusion of the gas through the film and release of the gas from solution in the low-pressure interface[1]. Therefore gas permeation is a rather complex process, which is strongly related to the thermodynamics of the polymer used as a gas barrier at a given temperature.

In the glassy state, the molecular chains are frozen and only local motions are permitted so that the development of holes through which molecules can jump is severely hindered. Moreover, owing to the fact that the glassy state is a metastable state, the permeability characteristics of the films depend on the sorption and thermal histories[2–7]. The packing efficiency of polymers with bulky functional groups is relatively low and the permeability of films prepared from these polymer chains is higher than that of films prepared from polymers with flexible chains.

Polymers in the rubbery state are similar to liquids in the sense that they respond quickly to external perturbations, in order to maintain thermodynamic equilibrium. Consequently, the permeation properties of polymer films made of these materials do not depend on the prior history. Diffusion is the rate-determining step in gas permeation, particularly at temperatures well above the glass transition temperature. As in the glassy state, the chemical structure governs the dynamics of the chains. Thus chains with bulky polar groups in their structure hinder long-range motions and, as a result, films made of these materials have a lower permeability in the rubbery state than other films in the same state prepared from polymers with more flexible molecular chains[8,9].

Owing to the close correlation between dynamics and diffusion, it is important to study the diffusional characteristics of polymer films in parallel with studies dealing with the influence of the orientation on the relaxation processes. Both gas permeation and relaxation processes are strongly dependent on the morphology of the films. For example, development of crystalline order reduces the solubility of the gases in the films, on

* To whom correspondence should be addressed

the one hand, and increases the tortuosity of the path followed by the diffusants in the matrix, on the other hand[10–12]. In the same way, the morphology also governs the relaxation behaviour of the films[13] so that it is extremely important to find out how molecular motions as determined by mechanical relaxation spectroscopy affect the diffusional characteristics of the films.

In a recent publication[14], the permeability properties and the mechanical relaxation behaviour exhibited by co-extruded linear low-density polyethylene (LLDPE) films were studied. It was found that the mechanical $\alpha$-relaxation, which is governed by molecular motions of the crystalline entities, seems to be the result of two overlapping peaks whose shape and location are dependent on the processing conditions of the films. Studies of the temperature dependence of both the permeability and diffusion coefficients over the range of temperatures where the $\alpha$-relaxation is located showed a strong sensitivity of these coefficients to the melting and recrystallization processes which occur in these films at high temperatures. These processes, reflected in the relaxation spectra, alter the morphology of the films and, as a result, their diffusional characteristics. The shape of the relaxation peaks and the permeation characteristics seem to be dependent on the orientation of the films. For this reason, attention is paid in this present work to the longitudinal and transverse responses of the co-extruded films in a dynamic mechanical force field.

Owing to the widespread use of co-extruded LLDPE films in the packaging industry, it was felt the need to investigate the diffusional characteristics of films of this kind which have been oriented by tensile drawing, either in the longitudinal or transverse directions. Therefore, in this present work the temperature dependence of both the permeability and diffusion coefficients of oxygen and carbon dioxide through these oriented LLDPE films are studied and the results compared with those corresponding to undrawn films.

## EXPERIMENTAL

### *Characteristics of the co-extruded films*

The films used in this study, which are basically copolymers of ethylene-*co*-octene with ca. 8 mol% of the latter comonomer, are made up of three layers, namely A (15 wt%), A (70 wt%), B (15 wt%), in which the layers A and B are, respectively, Dowlex/2247 ($\rho = 0.917\,g\,cm^{-3}$) and Dowlex/2291 ($\rho = 0.912\,g\,cm^{-3}$) (supplied by Dow Chemical, Tarragona, Spain).

The thermograms of the films, obtained with a Perkin-Elmer DSC-4 calorimeter at a heating rate of $8\,^{\circ}C\,min^{-1}$, exhibit a simple and broad melting peak, whose departures from the baseline and maximum are located, respectively, in the vicinity of 60 and 120°C. The degree of crystallinity of the films, determined by calorimetry, amounts to 25%. A more detailed analysis of the morphology of the films, carried out by using Raman spectroscopy, gives 0.24, 0.85 and 0.11 for the values of the crystalline, amorphous and crystalline–amorphous interface fractions, respectively. As a result of the processing conditions, the films are oriented in the direction of the extrusion (longitudinal direction), as indicated by their birefringence ($\Delta n = 1.4 \times 10^{-3}$).

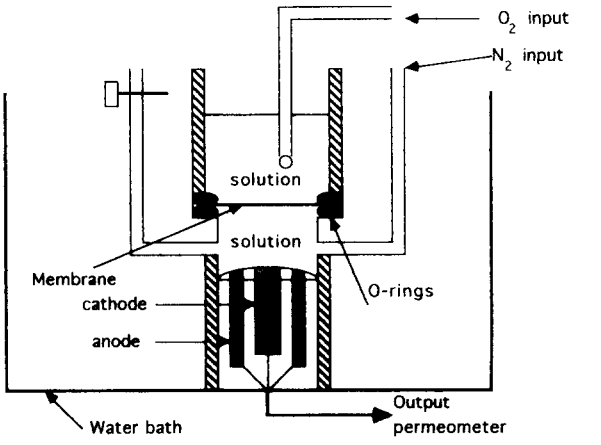


**Figure 1** Schematic diagram of the device used for permeability measurements of oxygen

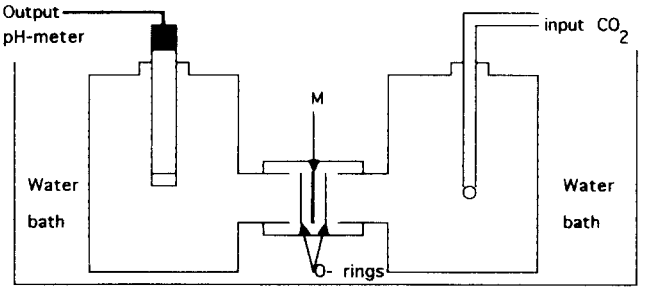


**Figure 2** Schematic diagram of the device used for permeability measurements of carbon dioxide

### *Permeability measurements*

The permeation of oxygen was measured in a cell made up of two chambers which are separated by the film whose permeability is being measured. One side of the film is in contact with an aqueous solution of oxygen whose pressure is 155 mmHg. The other side is separated from an oxygen electrode by a small cavity filled with deoxygenated distilled water. The electrode is a permeometer model 201 T (Rheder Development Co.) in which the polarographic cell is a solid cylindrical cathode of 24 carat gold (4.25 mm in diameter and 6 mm in length). The anode is a hollow cylinder made of silver (purity 99.9%), 7 mm in length with the internal and external diameter of the cylinder being 5 and 10 mm, respectively. The oxygen permeation was monitored by the oxygen electrode as indicated below. A thermistor was installed into the anode in order to monitor the temperature of the cell and the films during the permeation measurements. The temperature was controlled by a thermostated water bath which maintained the temperature to within $T \pm 0.1\,^{\circ}C$. Details of the experimental assembly are given in *Figure 1*[9].

The cell used for the permeation of carbon dioxide was made of Pyrex glass, designed specially for permeability measurements using the Orion-95-02 sensor. The film was clamped tightly between two compartments of approximately $150\,cm^3$ in capacity, while the surface area of the film through which permeation of the carbon dioxide took place was $4.15\,cm^2$. A diagram of the cell used is shown in *Figure 2*. The upstream side of the cell was filled with water saturated with $CO_2$ at a pressure of 1 atm, at time $t = 0$, and the pressure was kept constant

during the experiment. The downstream side of the cell contained water equilibrated with atmospheric $CO_2$ and the carbon dioxide sensor. Permeability coefficients were calculated from the change in concentration of $CO_2$, which was monitored by the $CO_2$ electrode. The experimental device was kept inside a water thermostat, and the accuracy of the temperature measurements was also ±0.1°C.

*Dynamic mechanical measurements*

Values of the storage relaxation modulus and the loss $\tan\delta$ of the films were measured at five frequencies (0.1, 0.3, 1, 3, and 10 Hz) with a PL-DMTA Mark II apparatus by using the double cantilever method in flexion mode. The measurements were performed from low to high temperatures, at a heating rate of $1°C\,min^{-1}$, over the temperature range from −140 to 100°C.

## PRINCIPLES OF OPERATION OF THE OXYGEN AND CARBON DIOXIDE SENSORS

The oxygen electrochemical device measures the cathodic current resulting from the following reaction:

$$\begin{aligned} O_2 + 2H_2O + 4e^- &\Leftrightarrow 4OH^- \\ 4Ag - 4e^- &\Leftrightarrow 4Ag^+ \end{aligned} \tag{1}$$

The flux of oxygen from the high-oxygen-concentration side of the membrane to the side facing the oxygen electrode, is assumed to obey Fick's law, as follows:

$$J = -D\frac{\partial C}{\partial x} = -Dk\frac{\partial p}{\partial x} \tag{2}$$

where $D$ is the diffusion coefficient, $C$ is the oxygen concentration in the solution, $x$ is the normal distance to the surface of the film, $p$ is the partial pressure of oxygen in the solution which is assumed to be related to the gas concentration by Henry's law ($C = kp$), and the product $kD$ is known as the permeability coefficient, $P$. Once the electrochemical process in the potentiostatic cell reaches steady-state conditions, the electrical current is related to the oxygen flux by the following relationship:

$$I(t \to \infty) = -\nu FAJ = \nu FA\frac{Dk}{L}(p_0 - p_L) \tag{3}$$

where $\nu$ is the number of electrons transferred in the cathodic reaction, $A$ is the area of the film facing the cathode, $F$ is the Faraday constant, $L$ is the thickness of the film and $p_0$ (= 155 mmHg) and $p_L$ are, respectively, the oxygen pressures on the two sides of the film. The oxygen permeating through the film is rapidly reduced by the cathode and, consequently, $p_L \sim 0$. Thus the permeability coefficient can be written as follows:

$$P = Dk = \frac{I(t \to \infty)L}{\nu FAp_0} \tag{4}$$

In order to determine the apparent diffusion coefficient of oxygen through the films, it is necessary to solve Fick's second law, i.e.

$$\frac{\partial p}{\partial t} = D\frac{\partial^2 p}{\partial x^2} \tag{5}$$

with the following boundary conditions:

$$\begin{aligned} p(x = 0,\ t < 0) &= 0 \\ p(x = 0,\ t \geqslant 0) &= p_0 \\ p(x = L,\ t \geqslant 0) &= 0 \end{aligned} \tag{6}$$

Solution of equation (5) gives[15] the oxygen partial pressure profile at time $t$, i.e. $p(x, t)$, which together with equation (2) and the expression $I = -\nu FAJ$ allows the determination of the diffusional characteristics of the films from electrochemical measurements. Thus the total electric charge transferred through the membrane in a time $t$ can be written as follows:

$$\begin{aligned} Q(t) &= \int_0^t I(\tau)\,d\tau \\ &= \nu FADk\int_0^t \left(\frac{\partial p}{\partial x}\right)_{x=0} d\tau \\ &= \nu FA\frac{Dk}{L}p_o\left(t - \frac{L^2}{6D}\right) \end{aligned} \tag{7}$$

The value of $D$ can be obtained from the intersect with the horizontal axis of the plot of $Q(t)$ against $t$. This procedure, also called the time-lag method, was used in the determination of the diffusion coefficient of oxygen through the LLDPE films.

The permeability of carbon dioxide was measured by utilizing an electrode sensor of Ag/AgCl in a liquid-to-liquid diffusion cell, similar to the oxygen sensor, in combination with a pH meter[16]. Carbon dioxide permeated through the membrane from the upstream side in which it was dissolved, at equilibrium, to the downstream side where the sensor is located, leading to the following reaction:

$$CO_2 + H_2O \Leftrightarrow HCO_3^- + H^+ \tag{8}$$

The permeation of $CO_2$ can be monitored by measuring the pH of the reaction medium, which is given by the following:

$$pH = pK + \log[HCO_3^-] - \log[CO_2] \tag{9}$$

where $pK = -\log K$, with $K$ being the dissociation constant of the reaction described in equation (8). By adding a small quantity of sodium bicarbonate, $[HCO_3^-]$ is kept constant, so that:

$$pH = A - \log[CO_2] \tag{10}$$

where $A = pK + \log[CO_3H^-]$. Changes of pH in the downstream chamber can be determined from the difference of the electromotive force $E$ with the reference electrode. Actually, $E$ is related to $[H^+]$ by the Nernst equation, as follows:

$$\begin{aligned} E &= E_0 + \frac{RT}{zF}\ln a_{H^+} \\ &= E_0 + \frac{RT}{zF}\ln\gamma + \frac{RT}{zF}\ln C_{H^+} \end{aligned} \tag{11}$$

where $\gamma$ is the activity coefficient and $z$ is the charge. By making

$$E_0' = E_0 + \frac{RT}{zF}\ln\gamma \tag{12}$$

and taking into account that $[CO_2] = [H^+]$, equation (11) can be written as follows:

$$E = E'_0 + \frac{RT}{zF}\ln[CO_2] \tag{13}$$

so that the concentration of carbon dioxide in the downstream chamber is given by:

$$[CO_2] = \exp\left(\frac{(E - E'_0)zF}{RT}\right) \tag{14}$$

The permeability of $CO_2$ can be determined by the procedure outlined by Nakagawa *et al.*[16]. Thus once steady-state conditions are reached, the permeation of gas through the membrane is expressed by the following relationship:

$$J = \frac{V}{A}\frac{dC}{dt} = Dk\left(\frac{p_0 - p_f}{L}\right) \tag{15}$$

where $V$ is the volume of the downstream chamber, $A$ is the area of the film through which permeation of the carbon dioxide takes place, and $p_0$ and $p_f$ are, respectively, the partial pressure of $CO_2$ at the high-stream and lowstream sides of the cell. By writing $p_f = C_f/\alpha$, where $\alpha$ is the Bunsen constant ($= 0.759\,cmHg^{-1}$ at 25°C), equation (15) leads to the following expression for the permeability:

$$P = Dk = L\left(\frac{dC}{dt}\right)\left(\frac{V}{A(p_0 - C_f/\alpha)}\right) \tag{16}$$

where $dC/dt$ was obtained from equation (14). The diffusion coefficient of $CO_2$ was determined by the lag-time method.

## RESULTS

### *Mechanical relaxation spectra*

As indicated in the Experimental section, the processing conditions confer orientation to the films. With the aim of obtaining information on how the orientation can affect the dynamic mechanical behaviour of the films, pertinent experiments were performed on the films in parallel ($_{\|}$) and transverse ($_{\perp}$) directions to the processing orientation. In the following, the physical properties thus measured will carry these symbols as subindices.

The dynamic mechanical results, expressed in terms of both $\tan\delta_{\|}$ and $\tan\delta_{\perp}$, are represented as a function of the temperature in *Figure 3*. In both cases, the relaxation spectra present three absorptions, which going from low to high temperature are denoted as the $\gamma$- $\beta$- and $\alpha$-relaxation processes. Whereas the $\gamma$-relaxation is a well-defined peak, the $\beta$-process overlaps with the $\alpha$-relaxation, appearing as a shoulder of the latter absorption. However, if the results corresponding to the $\beta$-region are expressed in terms of the loss relaxation modulus, the $\beta$-peak becomes a well-defined relaxation process, as indicated in *Figure 4*, where the values of $E''_{\|}$ as a function of temperature are shown. The $\beta$-process does not show a noticeable dependence on the orientation, as can be seen in *Figure 5* where the temperature dependence of $E''_{\perp}$ and $E''_{\|}$ at 1 Hz is represented.

The $\alpha_{\|}$ absorption seems to be formed by a poorly defined $\alpha'$-peak in the low-temperature side of this relaxation, followed by an ostensible $\alpha''$-peak; as can be seen in *Figure 6*, only the $\alpha'$-peak is detected in the measurements performed in the direction transverse to the processing direction.

### *Permeability and diffusion coefficients*

Values, measured at different temperatures, of the permeability coefficients of $O_2$ and $CO_2$ through the undrawn films are shown in *Figures 7* and *8*, where three well-differentiated regions can be detected. In the first region, extending from 20 to 35°C, the permeability of oxygen is an increasing linear function of temperature; at ~35°C, a comparatively steep increase in the permeability occurs, reaching a plateau at ~40°C. The

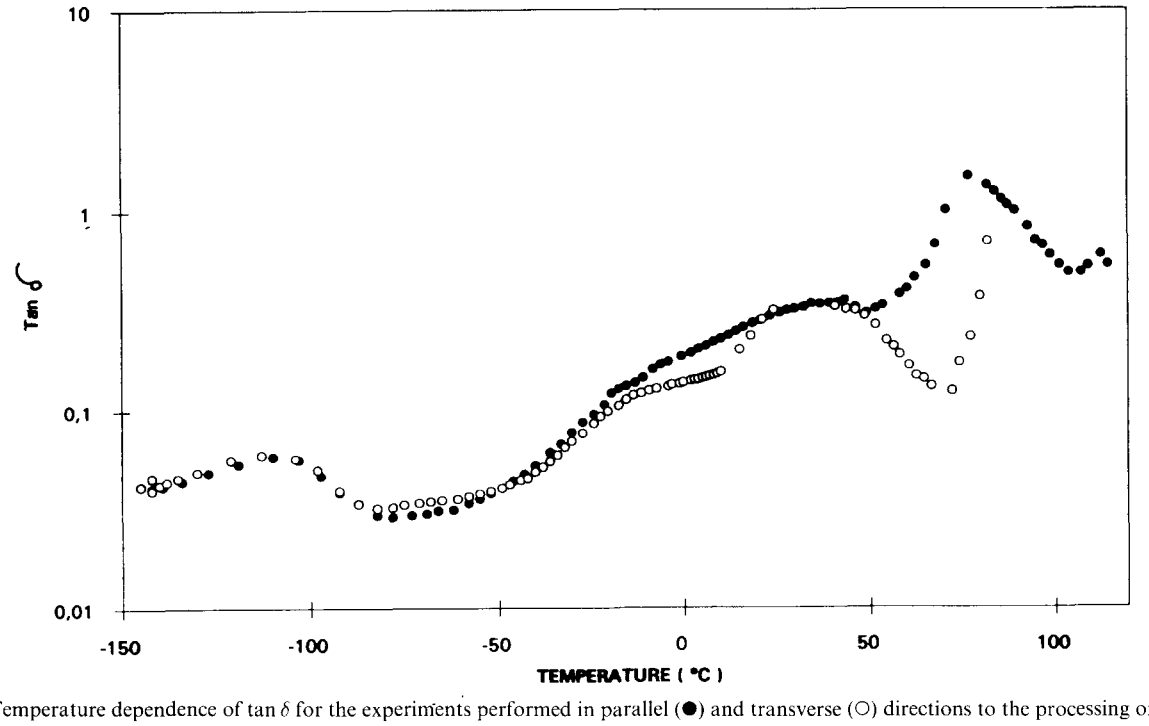


**Figure 3** Temperature dependence of tan $\delta$ for the experiments performed in parallel (●) and transverse (○) directions to the processing orientation

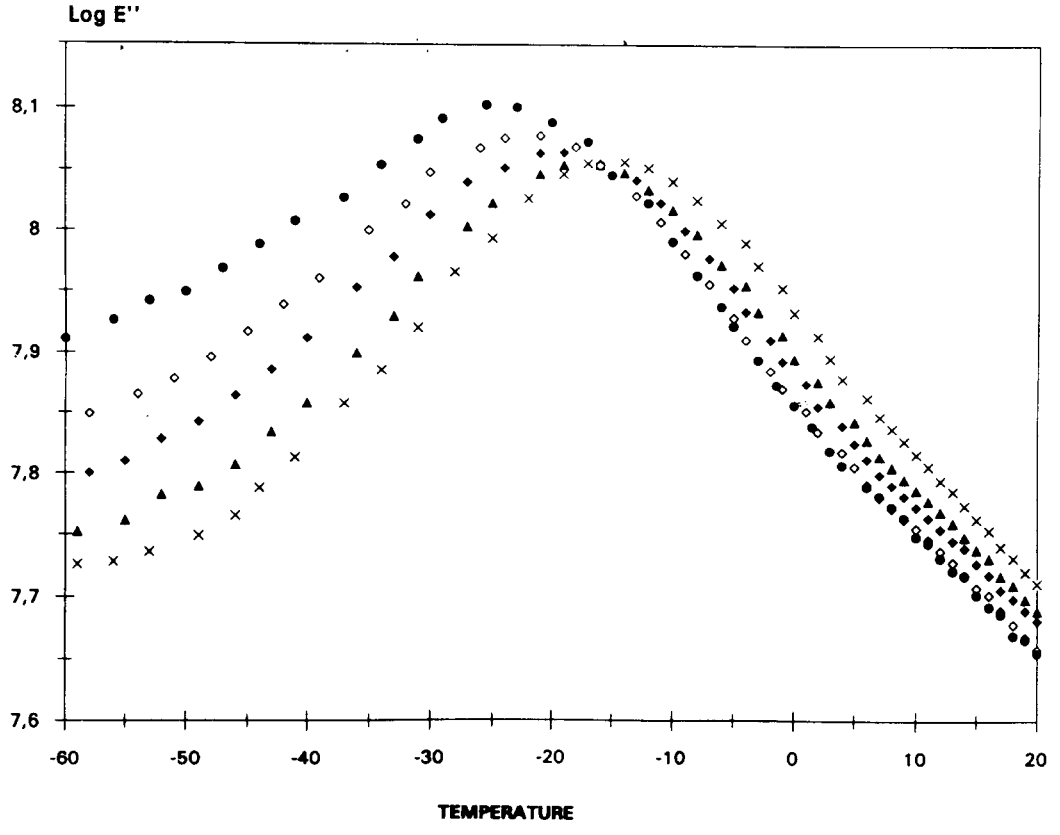


**Figure 4** Variation of the loss relaxation modulus (Pa) with temperature in the $\beta$-region. The results were obtained in a parallel direction to the processing orientation at the following frequencies: (●) 0.1; (◇) 0.3; (◆) 1; (▲) 3; (×) 10 Hz

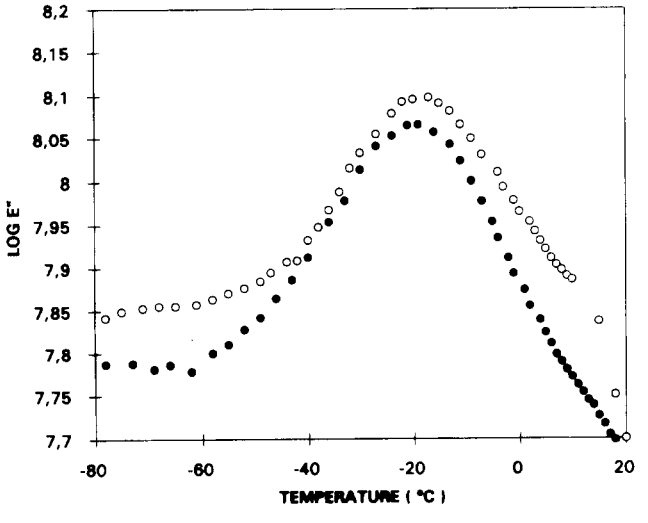


**Figure 5** Temperature dependence of the loss relaxation modulus (Pa) in the $\beta$-region; the results were obtained at 1 Hz in parallel (●) and transverse (○) directions to the processing orientation

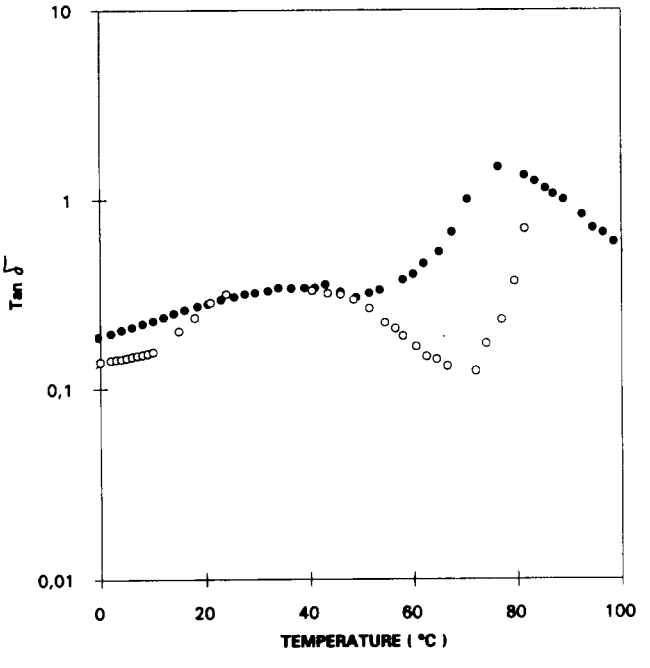


**Figure 6** Temperature dependence of tan $\delta$ in the $\alpha$-region; filled and open symbols refer, respectively, to results obtained in paralle and transverse directions to the processing orientation

temperature dependence of the permeability coefficient of $CO_2$ follows similar trends although, as is usually observed, this coefficient is much larger than that of oxygen.

The permeability coefficient was also obtained for oriented films by tensile drawing in which the elongation ratio ($\lambda_{\|}$) in the direction parallel to the processing orientation was 2; these experiments were also performed on oriented films after drawing in a direction perpendicular to the processing orientation, for which the elongation ratio ($\lambda_{\perp}$) was also 2. Although the temperature dependence of $P_{\|}$ exhibits three regions, as in the case of the undrawn films, the increase in the permeability coefficient between the first and third region is relatively small. The results of *Figure 6* show, for

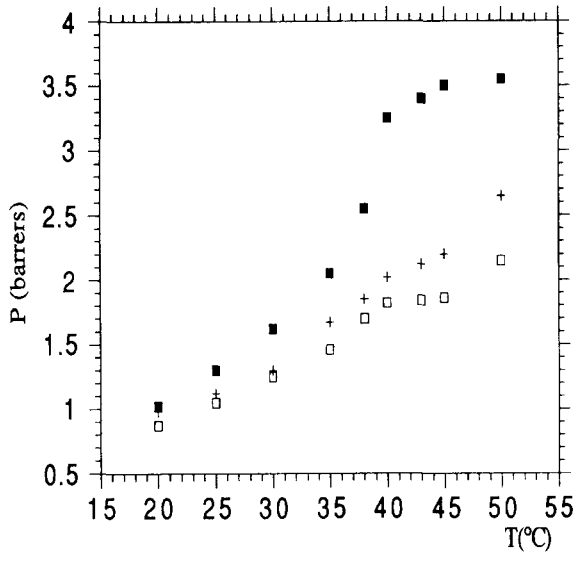


**Figure 7** Plots showing the permeability coefficient of oxygen through co-extruded LLDPE films (■) and through films tensile drawn in parallel (□) and transverse (+) directions to the processing orientation; in the latter two cases the elongation ratio was 2

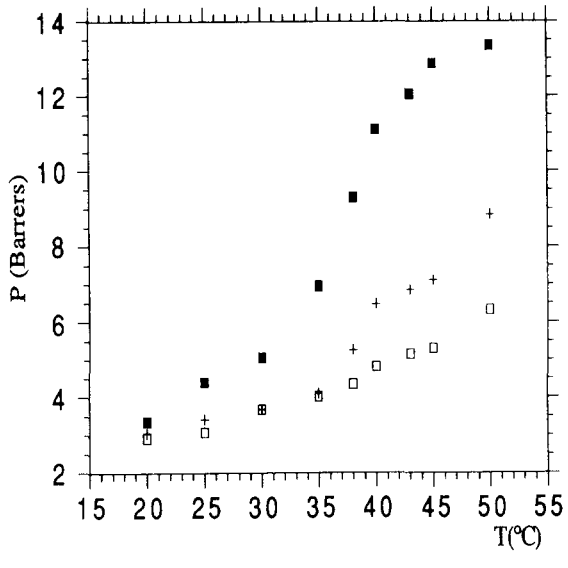


**Figure 8** Plots showing the permeability coefficient of carbon dioxide through co-extruded LLDPE films (■) and films tensile drawn in parallel (□) and transverse (+) directions to the processing orientation; in the latter two cases the elongation ratio was 2

example, that the value of $P$ for $CO_2$ through the undrawn film in the plateau region is ca. 13 Barrer at 50°C, whereas the value for $P_{\|}$ is only 6 Barrer at the same temperature. As can be seen in *Figures 7* and *8*, the temperature dependence of both $P_{\|}$ and $P_{\perp}$ in the first region is similar; departure of the values of these quantities from those corresponding to the undrawn films appears in the second and third regions, with the values of $P_{\perp}$ being somewhat larger than those of $P_{\|}$.

The results for the diffusion coefficients of oxygen and carbon dioxide through the tensile undrawn films, $D$, are represented in *Figures 9* and *10*, respectively. The values of $D_{\|}$ and $D_{\perp}$ are plotted in the same figures, where it can be seen that relatively strong changes of the diffusion coefficients with temperature, compared to those taking place with the permeability coefficients, do not occur.

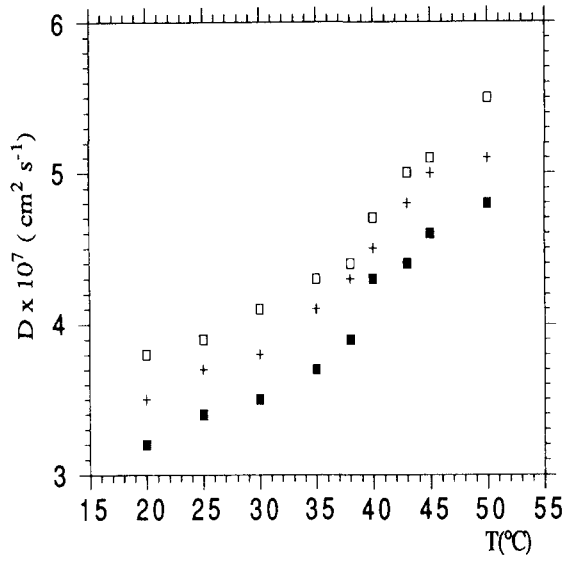


**Figure 9** Variation of the diffusion coefficient of oxygen through co-extruded LLDPE films (+) and through films tensile drawn in parallel (□) and tranverse (■) directions to the processing orientation. (The plot showing the temperature dependence of th diffusion coefficient of oxygen for undrawn LLDPE films in figures 2 and 3 of ref. 14, should read D × $10^7$ $cm^2$ $s^{-1}$ instead of D × $10^8$ $cm^2$ $s^{-1}$ on the ordinate axis)

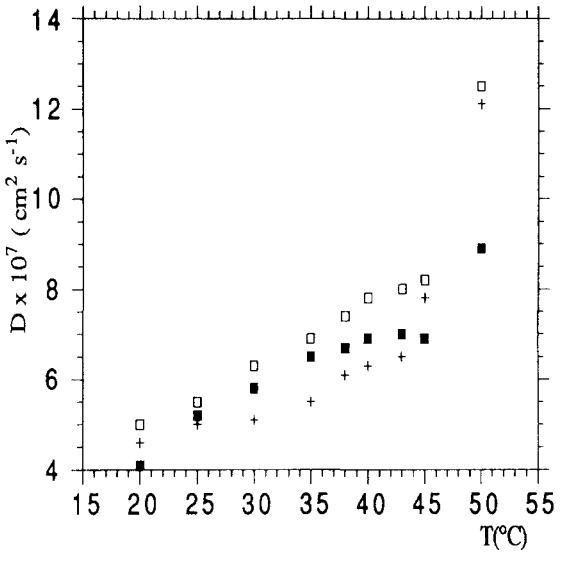


**Figure 10** Variation of the diffusion coefficient of carbon dioxide through co-extruded LLDPE films (+) and films tensile drawn in parallel (□) and transverse (+) directions to the processing orientation. (The plot showing the temperature dependence of the diffusion coefficient of carbon dioxide for undrawn LLDPE films in figures 2 and 3 of ref. 14, should read D × $10^7$ $cm^2$ $s^{-1}$ instead of D × $10^8$ $cm^2$ $s^{-1}$ on the ordinate axis)

## DISCUSSION

In general, the mechanical relaxation spectra of polyethylene present three transitions, denoted as $\alpha$, $\beta$, and $\gamma$, in order of decreasing temperature. In addition it is a well-stated fact that the location and intensity of the peaks depend on the morphology and branching of the samples[13,17]. The $\gamma$-transition seems to have its origin in the amorphous regions and most researchers seem to agree that the process involves a cooperative short-range conformational transition requiring a minimum of three

skeletal bonds. Actually, simulation studies carried out by Helfand and coworkers on local motions that produce secondary relaxations in simple chains such as polyethylene indicate that the following transitions[18]:

$$\begin{aligned} \ldots g^{\pm}tt\ldots &\Leftrightarrow \ldots ttg^{\pm}\ldots \\ \ldots ttt\ldots &\Leftrightarrow \ldots g^{\pm}tg^{\mp}\ldots \end{aligned} \qquad (17)$$

overwhelmingly account for the cooperativity. In both cases, the final state of each bond, except the central one, is parallel to its initial position; this parallel transition will also occur with the molecular tails attached to the bonds that undergo these transitions.

The $\beta$-relaxation is weak for high-density polyethylene, but it becomes a well-developed process in branched polyethylene. Although the origin of this relaxation still needs to be clarified, the fact that the intensity of the relaxation process increases as the branching increases led to it being attributed to motions of branches in the amorphous matrix[19–21]. Therefore linear low-density polyethylene exhibits a $\beta$-relaxation whose intensity increases as the comonomer (1-octene, 1-butene, etc.) content increases. Although some studies seem to indicate that the $\beta$-absorption exhibits the characteristics of a glass–rubber relaxation, analysis of the normal Raman modes suggest that it may result from motions of disordered chain units associated with the interfacial regions of semicrystalline polyethylene[22]. Finally, the $\alpha$-transition increases with crystallinity and therefore it was attributed to molecular motions in which crystalline entities intervene[19,23,24]. The fact, however, that this transition is not observed in the mechanical relaxation spectrum of single crystals of n-alkanes[25] indicates that the presence of an amorphous region is necessary for its development. In accord with this, Boyd[26] has attributed the $\alpha$-relaxation to the deformation of the amorphous region, which takes place as a consequence of reorientation within the crystallites.

The effects of the orientation on the relaxation behaviour of the films was studied by registering the mechanical spectrum in directions longitudinal and transverse to the processing orientation. Both spectra nearly superpose in the $\gamma$- and $\beta$-regions, thus indicating that the orientation does not have a noticeable influence in these processes. However, a clear difference can be detected in the $\alpha$-region, as can be seen in *Figure 6* where the $\alpha$-peaks obtained in the longitudinal and transverse experiments are represented. For example, the $\alpha$-peak corresponding to the longitudinal experiments seems to be the result of a broad and poorly defined $\alpha'$-peak, centred at ca. 80°C. Since an increase in the storage relaxation modulus is detected in the region where the $\alpha''$-peak is located, this relaxation process was attributed to crystallites thickening. The results obtained in the transverse experiments only exhibit a relatively well-defined $\alpha'$-peak which is centred at the same temperature as the $\alpha'$-peak which corresponds to the longitudinal experiments.

The temperature dependence of the permeability of $O_2$ and $CO_2$ through undrawn films show three well-differentiated regions in the temperature interval between 20 and 50°C, with the changes in $P$ in these regions when going from low to high temperature being, respectively, moderately low, high and virtually zero. It is noteworthy that this apparently complex permeation behaviour occurs in the temperature interval where the $\alpha'$-peak develops. The decrease in the permeation coefficient with orientation which is observed in *Figures 7* and *8* may be due either to a diminution of the solubility coefficient in the oriented films as a result of tensile drawing, or to an increase of the tortuosity factor in these films which affects the ease of gas diffusion. One would expect that tensile drawing would increase conformational order in the crystalline–amorphous interphase, thus decreasing the diffusion coefficient. However, the curves representing the temperature dependence of the diffusion coefficient (*Figures 9* and *10*) do not follow similar trends. Thus the values of $D$ for $O_2$ and $CO_2$ through undrawn LLDPE films are, respectively, intermediate to and lower than those found for this parameter for the films oriented by tensile drawing. At first sight, the decrease observed in the values of the permeability coefficient with drawing might seem consistent with earlier results reported by Ward and coworkers[12] for highly oriented polyethylene. The reduction in the permeability characteristics of drawn polyethylene was attributed by these authors to the fact that, on drawing, the initial spherulitic structure transforms into a new microfibrilar structure. In drawing, microshear processes at the surface of the fibrils may produce extended molecules and also the possibility could exist of an improvement in molecular order in the crystalline–amorphous interface. However, the only minor changes that drawing introduces in the gas diffusion coefficients through the films used in this study suggest that morphological transformation, if any occur, would have a greater effect on the solution–film interface, and hence the solubility coefficient, than on the diffusion paths of the films.

The permeation properties in amorphous films are thermally activated processes, i.e. their temperature dependence follows an Arrhenius-type behaviour. Consequently, apparent activation energies associated with these processes are determined from semilogarithmic plots of the permeation and diffusion coefficients against the reciprocal of the absolute temperature. The situation can be somewhat more complex in semicrystalline polymers, as is shown in *Figures 11* and *12* where plots

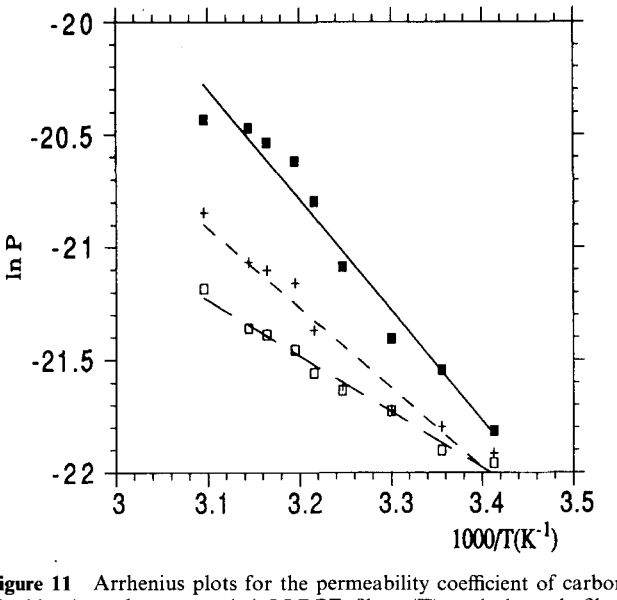


**Figure 11** Arrhenius plots for the permeability coefficient of carbon dioxide through co-extruded LLDPE films (■) and through films tensile drawn in parallel (□) and transverse (+) directions to the processing orientation

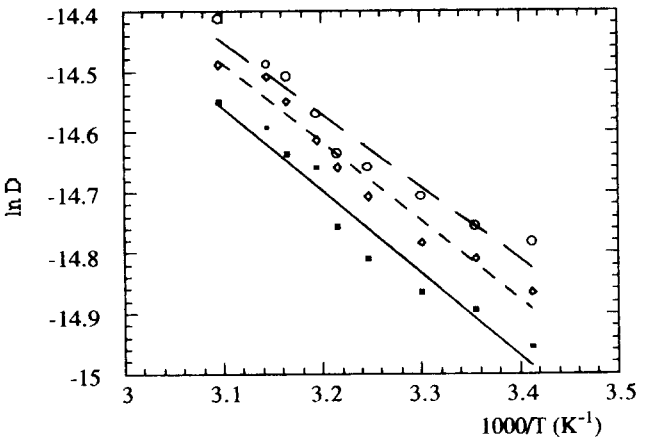


**Figure 12** Arrhenius plots for the diffusion coefficient of oxygen through co-extruded LLDPE films (◇) and through films tensile drawn in parallel (■) and transverse (○) directions to the processing orientation

**Table 1** Values of the activation energies (kcal mol$^{-1}$) associated with the apparent permeability and diffusion coefficients for $O_2$ and $CO_2$ through unstrained films and films oriented by tensile drawing over the temperature range from 290 to 320 K

| | Carbon dioxide | | Oxygen | |
|---|---|---|---|---|
| Gas barrier | $E_P$ | $E_D$ | $E_P$ | $E_D$ |
| Undrawn film | 9.8 | 5.0 | 8.9 | 2.6 |
| Tensile-drawn film ($\lambda_{\parallel} = 2$) | 4.9 | 4.0 | 5.9 | 2.6 |
| Tensile-drawn film ($\lambda_{\perp} = 2$) | 7.0 | 4.8 | 6.4 | 2.4 |

of this kind are presented. It can be seen that the fitting of the experimental results to straight lines is rather poor for the permeability coefficient of the undrawn films, but is somewhat better in the oriented films produced by tensile drawing. Values of the apparent activation energies associated with the permeability coefficients are presented in *Table 1*. The discrepancies observed for the activation energies of the permeability coefficients may be the result of differences in the solubility coefficients brought about by the effects of orientation.

The Arrhenius plots for the diffusion coefficient also correspond rather poorly to straight lines. It is noteworthy that the apparent activation energies associated with the diffusion coefficients seem to be independent of tensile drawing, thus suggesting that the diffusion paths may not be significantly affected by the orientation.

## CONCLUSIONS

The location and shape of the $\gamma$- and $\beta$-mechanical relaxations in LLDPE films do not seem to be dependent on the orientation of the films. The $\alpha$-relaxation is sensitive to the orientation as a consequence of the fact that it arises from motions in which crystalline entities intervene.

In general orientation decreases the permeability coefficients of oxygen and carbon dioxide through the LLDPE films. The fact, however, that the corresponding effect on the diffusion coefficient seem to be relatively small suggests that changes in the solution–film interface, rather than in the diffusion coefficients, are responsible for the decrease in permeability observed in LLDPE films which have been oriented by tensile drawing.

## REFERENCES

1 Stern, S. A., Sampat, S. R. and Kulkarni, S. S. *J. Polym. Sci. Polym. Phys. Edn* 1986, **24**, 2149
2 Kim, T. H., Koros, W. J. and Husk, G. R. *Sep. Sci. Technol.* 1988, **23**, 1611
3 Stern, S. A., Mi, Y., Yamamoto, H. and St. Clair, A. K. *J. Polym. Sci. Polym. Phys. Edn* 1989, **27**, 1887
4 Hoehn, H. H. in 'Materials Science of Synthetic Membranes' (Ed. D. R. Lloyd), ACS Symposium Series No. 269, American Chemical Society, Washington, DC, 1985, p. 85
5 Tanaka, K., Kita, H., Okamoto, K., Nakamura, A. and Kusuki, Y. *Polym. J.* 1990, **22**, 381
6 Tanaka, K., Kita, H., Okano, M. and Okamoto, K. *Polymer* 1992, **33**, 585
7 Tanaka, K., Okano, M., Toshina, H., Kita, H. and Okamoto, K. *J. Polym. Sci. Polym. Phys. Edn.* 1992, **30**, 907
8 Sonnenburg, J., Gao, G. J. and Weiner, H. *Macromolecules* 1990, **23**, 4653
9 Campañ, V., Riande, E., San Román, J. and Díaz-Calleja, R. *Polymer* 1993, **34**, 3843
10 Michaels, S. A. and Bixler, H. *J. Polym. Sci.* 1959, **41**, 53
11 Michaels, S. A. and Bixler, H. *J. Polym. Sci.* 1960, **50**, 393
12 Holden, P. S., Orchard, G. A. J. and Ward, I. M. *J. Polym. Sci. Polym. Phys. Edn* 1985, **23**, 709
13 McCrum, N. G., Read, B. E. and Williams, G. 'Anelastic and Dielectric Effects in Polymeric Solids', Wiley, London, 1967
14 Compañ, V., Ribes, A., Riande, E. and Díaz-Calleja, R. *Polymer* 1995, **36**, 323
15 Carslow, H.S. and Jaeger, J. C. 'Conduction of Heat in Solids', Oxford University Press, Oxford, 1959, p. 313
16 Nakagawa, T., Naruse, A. and Higuchi, A. *J. Appl. Polym. Sci.* 1992, **42**, 383
17 Khanna, Y. P., Turi, E. A., Taylor, J., Vickroy, V. V. and Abbott, F. *Macromolecules* 1985, **18**, 1302
18 Helfand, H. *Science* 1984, **226**, 647
19 Stehling, F. C. and Mandelkern, L. *Macromolecules* 1970, **3**, 242
20 Kline, D. E., Saever, J. A. and Woodward, A. E. *J. Polym. Sci.* 1956, **22**, 455
21 Clas, S.-D., McFadding, D. C. and Russell, K. E. *J. Polym. Sci. Polym. Phys. Edn* 1987,**26**, 1057
22 Popli, R., Glotin, M., Mandelkern, L. and Benson, R. L. *J. Polym. Sci. Polym. Phys. Edn* 1984, **22**, 407.
23 McCrum, N. G. in 'Molecular Basis of Transitions and Relaxations' (Ed. D. J. Meier), Gordon and Breach, New York, 1978, p. 167
24 Boyd, R. F. *Rubber Rev.* 1963, **36**, 1303
25 Crismann, J. M. *J. Polym. Sci. Polym. Phys. Edn* 1975, **13**, 1407
26 Boyd, R. H. *Polym. Eng. Sci.* 1979, **19**, 1010